Signatures of attosecond electron tunneling dynamics in the evolution of intense few-cycle light pulses

E. E. Serebryannikov,[1] A. J. Verhoef,[2] A. Mitrofanov,[2] A. Baltuška,[2] and A. M. Zheltikov[1]
[1]*Physics Department, International Laser Center, M.V. Lomonosov Moscow State University, Vorobyevy Gory, 119992 Moscow, Russia*
[2]*Photonics Institute, Vienna University of Technology, Gusshausstrasse 27-387, A-1040 Vienna, Austria*
(Received 27 March 2009; published 9 November 2009)

The sensitivity of electron tunneling to the phase of an ionizing light field is shown to manifest itself in detectable features in the spectral and temporal evolution of intense few-cycle light pulses in an ionizing medium. An ultrafast buildup of electron density in the regime of tunneling ionization gives rise to a modulation of a few-cycle field wave form and enhances the short-wavelength part of its spectrum. In a low-pressure gas, the signatures of electron tunneling in the evolution of few-cycle pulses can be isolated from the effects related to atomic nonlinear susceptibilities, giving an access to attosecond electron tunneling dynamics.

DOI: 10.1103/PhysRevA.80.053809 PACS number(s): 42.65.Ky

I. INTRODUCTION

Ionization is one of the key physical phenomena in the interaction of intense light fields with matter. Ionization effects play a significant role in nonlinear-optical transformations of intense ultrashort light pulses, contributing to a spatial, temporal, and spectral dynamics of a laser field through spectral blue shifting, beam defocusing, and pulse reshaping [1,2]. Nonlinear optics of ionizing media involves a rich variety of interesting and practically significant phenomena, such as optical harmonic [3] and supercontinuum (SC) [4–6] generation, filamentation [1,2,7], and generation of terahertz radiation [8,9]. This class of nonlinear-optical interactions enables advanced lightwave technologies [10], including attosecond pulse generation [11], transmission of high-peak-power laser signals through the atmosphere [12], carrier-envelope phase control of few-cycle field wave forms [13], as well as conversion of visible and infrared radiation to ultrashort pulses of coherent uv [14,15] and x-ray radiation [3,11].

Modeling of nonlinear-optical transformations of high-intensity ultrashort pulses in ionizing media [1,2,16,17] usually involves solving an envelope or field-evolution equation including dispersion effects, Kerr, Raman, and ionization nonlinearities, as well as diffraction and spatial self-action phenomena. Ionization dynamics is included in this model through Keldysh-type formulas [18] for the ionization rate. This approach, as shown in an extensive literature (see, e.g., Refs. [1,2] for review), provides an adequate description of many significant tendencies in the temporal, spectral, and spatial evolution of ultrashort light pulses, including compression to few-cycle pulse widths. However, standard Keldysh-type expressions define ionization rates averaged over the field cycle. The sensitivity of the ionization rate to the phase of a laser field is thus lost with such an approach. In high-intensity fields, however, an ionization process is typically dominated by electron tunneling. In this regime, it takes an electron only a fraction of a field cycle to tunnel through a field-modified potential barrier. As a result, the buildup of electron density becomes highly sensitive to the phase of the laser field [19].

Here, we show that, in the regime of tunneling ionization, spectral and temporal evolution of intense few-cycle light pulses may noticeably deviate from predictions of models using cycle-averaged ionization rates. Electron tunneling induced by a few-cycle light pulse gives rise to a stepwise modulation of the electron density, with each step in electron density buildup locked to a field half-cycle with an attosecond precision. We demonstrate below that this effect translates into an ultrafast modulation of the field envelope and gives rise to intense odd-harmonic generation.

II. NUMERICAL MODEL

For a numerical analysis of the spatiotemporal evolution of high-intensity ultrashort field wave forms in a fast-ionizing gas medium, we use the framework of the slowly evolving wave approximation (SEWA) [3,20], adapted to include ionization effects [16,17]. This SEWA-based model, which has been discussed in an extensive literature (see, e.g., Refs. [1,2] for a review), includes dispersion of the gas medium and plasma dispersion, diffraction, Kerr-effect-induced spatial and temporal self-action of the laser field, as well as ionization-induced loss and nonlinear-optical effects, involving a numerical solution of the following equation for the evolution of the field E,

$$\begin{aligned}\frac{\partial E(z,r,\omega)}{\partial z} &= -\frac{1}{2}\hat{F}\left\{\frac{I_p}{I(z,r,t)}\frac{\partial n_e(z,r,t)}{\partial t}E(z,r,t)\right\} \\ &+ i\sum_{n=2}^{\infty}\frac{(\omega-\omega_o)^n}{n!}\left.\frac{\partial^n k}{\partial\omega^n}\right|_{\omega_o}E(z,r,\omega) \\ &+ i\frac{1}{2k(\omega)}\left[\frac{\partial^2}{\partial r^2}+\frac{\partial}{r\,\partial r}\right]E(z,r,\omega) \\ &+ i\frac{\mu_o\omega^2}{2k(\omega)}P_{NL}(z,r,\omega) \\ &- i\frac{\mu_o}{2k(\omega)}\frac{e^2}{m_e}\hat{F}\{E(z,r,t)n_e(z,r,t)\}. \qquad (1)\end{aligned}$$

Here, $E(z,r,\omega)=\hat{F}(\frac{1}{2}E(z,r,t)\exp(i\omega_0 t)+\text{c.c.})$, $\hat{F}(\cdot)$ is the Fourier transform operator, $E(z,r,t)$ is the field envelope, z and r are the longitudinal and radial coordinates, respec-

tively, ω_0 is the central frequency of the laser field, $P_{NL}(z,r,\omega)$ is the Fourier transform of the time-domain nonlinear polarization related to the atomic nonlinear susceptibilities of the medium. Dispersion of the gas medium is plugged into Eq. (1) through the frequency profile of the wave number $k=k(\omega)$, which automatically includes high-order dispersion effects.

To complete the model, we supplement the field-evolution equation [Eq. (1)] with an equation governing the buildup of the electron density n_e: $\partial n_e/\partial t=w(n_0-n_e)$. Here, w is the ionization rate and n_0 is the initial density of neutral species. In earlier work, ionization effects have been included in the field-evolution equation through Keldysh-type formulas, allowing a calculation of the field-cycle-averaged ionization rate. However, in a high-intensity field [understood here as a field E such that the Keldysh parameter $\gamma=\omega(2m_eI_p)^{1/2}(eE)^{-1}$ is less than unity, I_p being the ionization potential, and e and m_e being the electron charge and mass], electron tunneling starts to dominate ionization process. With electron tunneling occurring on a time scale less than the field cycle, the sensitivity of the ionization rate to the phase of the laser field needs to be included in the ionization model for an accurate description of ionization effects. Here, we extend the analysis of the evolution of high-intensity few-cycle pulses in fast-ionizing media to the regime of phase-sensitive tunneling ionization by combining the field-evolution equation with a formalism allowing the ionization rate $w(t)$ to be calculated as a function of the instantaneous field amplitude without averaging over the field cycle.

In the regime of small Keldysh parameters, $\gamma \ll 1$, field-phase-sensitive effects in nonlinear-optical phenomena can be analyzed, as convincingly shown by the earlier work (see, e.g., Refs. [21,22]), by using the quasistatic-approximation nonadiabatic Ammosov-Delone-Krainov-type (ADK) formulas [23], involving the instantaneous rather than cycle-averaged field intensity,

$$w_{qs}(t)=\omega_p|C_{n^*}|^2\left(\frac{4\omega_p}{\omega_t}\right)^{2n^*-1}\exp\left(-\frac{4\omega_p}{3\omega_t}\right), \qquad (2)$$

where $\omega_p=I_p/\hbar$, $\omega_t=e|E(t)|(2m_eI_p)^{-1/2}$, $n^*=Z(I_H/I_p)^{1/2}$, $|C_{n^*}|^2=2^{2n^*}[n^*\Gamma(n^*+1)\Gamma(n^*)]^{-1}$, Z is the atomic net charge and I_H is the ionization potential of the hydrogen atom.

However, in the intermediate range, where γ is on the order of unity, which is often the case in filamentation and SC generation experiments, as well as in the multiphoton regime, where $\gamma>1$, the approximation of Eq. (2) is, rigorously speaking, inapplicable. If Eq. (2) is applied arbitrarily without any modification of its form to the $\gamma>1$ range, the ionization rate would remain sensitive to the phase of the laser field, which is an unphysical result. This issue has been addressed by Yudin and Ivanov [19], who derived a closed-form analytical expression for the ionization rate applicable for arbitrary γ. The Yudin-Ivanov (YI) formula has been shown [24] to agree well with the Schrödinger-equation analysis of ionization. With cycle averaging, on the other hand, the YI formula reproduces Keldysh-type expressions for the ionization rate [19], thus suggesting an adequate model also for multiphoton ionization. In Figs. 1(a)–1(d), we compare predictions of the YI formula and the quasistatic approach based on Eq. (2) for the ionization rate calculated as a function of the phase φ of the field intensity $I(\varphi)\propto\cos^2\varphi$ within a field intensity half-cycle (shown by the dashed line) for different values of the Keldysh parameter γ. As can be seen from this comparison, both approaches give nearly identical results in the regime of small γ [Fig. 1(a)]. However, as γ increases, predictions of these two models tend to diverge [cf. the solid and dash-dotted lines in Figs. 1(b)–1(d)]. While the quasistatic approximation predicts stronger localized peaks in $w(\varphi)$ around $\varphi=0$, the YI formula correctly recovers transition to the regime of multiphoton, where the ionization rate should display no or weak sensitivity to the phase of the field.

Figures 2(a) and 2(b) compare the buildup of the electron density n_e simulated by solving the equation $\partial n_e/\partial t=w(n_0-n_e)$ in the case of a few-cycle laser pulse, with the ionization rate $w(t)$ calculated by using three different approaches—the YI formula, Keldysh-type, Popov-Perelomov-Terentyev (PPT) formula [25], and the quasistatic-approximation nonadiabatic ADK-type expression (2). In agreement with expectations based on the comparison of $w(\varphi)$ calculations performed with different approaches [Figs. 1(a)–1(d)], the YI formula and the quasistatic approximation give nearly identical results for the $n_e(t)$ profile in the $\gamma<1$ regime [cf. the solid and dash-dotted curves in Fig. 2(a)]. These predictions, however, drastically differ from the results of calculations using the PPT formula, which involves averaging over the field cycle in calculation of the ionization rate. While the PPT formula predicts a smooth buildup of the electron density [the dashed line in Figs. 2(a) and 2(b)], the time dependences of n_e calculated with the use of the YI formula and the quasistatic approximation display a steplike behavior, reflecting the sensitivity of the ionization rate to the phase of the laser field. Indeed, with $n_e \ll n_0$, one finds $n_e(t)=n_0\int_{-\infty}^{t}w(\xi)d\xi$, showing that each step in the $n_e(t)$ profile is locked to a respective field intensity half-cycle. Such a behavior of $n_e(t)$ has been known from the earlier theoretical work (see Refs. [3,26] for an overview) and has been recently visualized experimentally by time-of-flight spectrometry measurements [24], where attosecond steps in the ion yield have been resolved by using an isolated xuv attosecond pump pulse and a few-cycle optical probe pulse. In the spectral domain, a stepwise modulation of the electron density has been shown to induce optical harmonic generation [27]. Optical harmonics of this type have been recently isolated in noncollinear pump-probe experiments with a few-cycle pump field [28]. In the time domain, a stepwise modulation of the electron density gives rise to an ultrafast amplitude and phase modulation of an optical field, leading to new effects in the spectral and temporal evolution of intense few-cycle light pulses.

As one could also expect from the comparison of $w(\varphi)$ dependences in Figs. 1(a)–1(d), predictions of the YI formula and the quasistatic approximation tend to diverge in the transient regime, where γ is on the order of unity, and in the regime of multiphoton ionization, with $\gamma>1$ [see Fig. 2(b)]. As γ increases, ionization steps in the $n_e(t)$ profiles

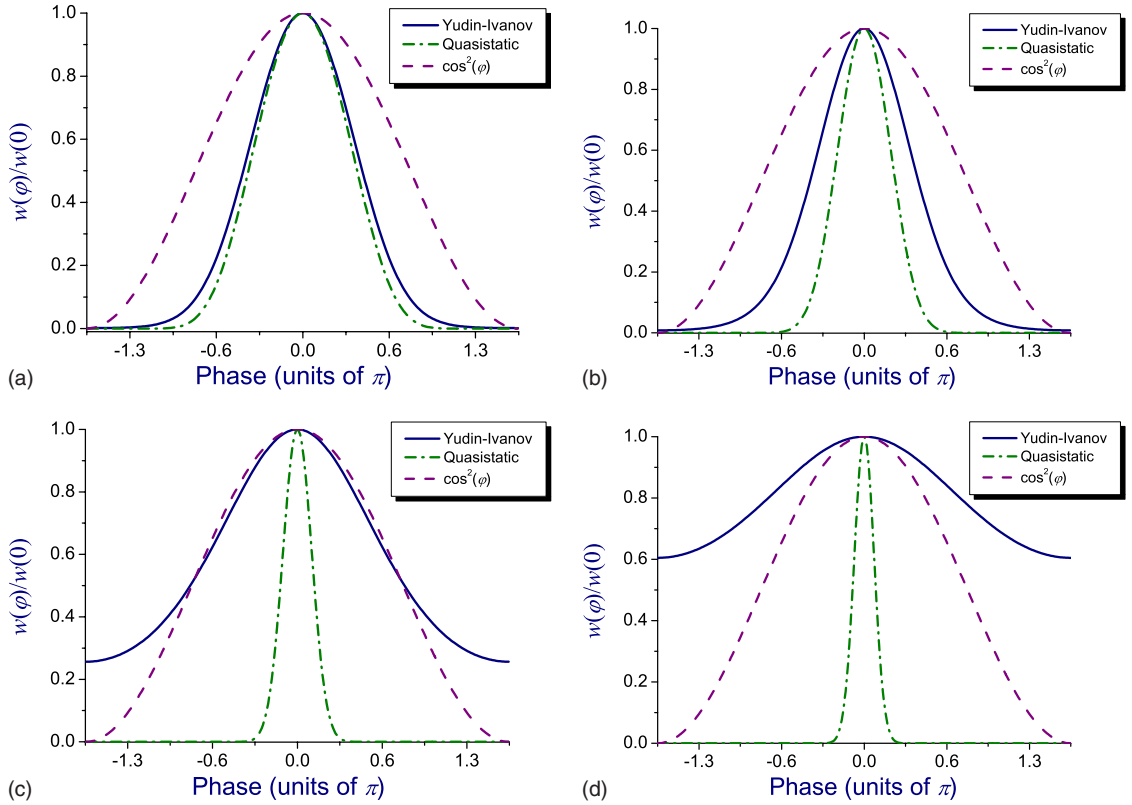

FIG. 1. (Color online) The ionization rate as a function of the phase φ of the light field within a field half-cycle (shown by the dashed line) calculated by using the Yudin-Ivanov (solid line) formula and the quasistatic approximation of Eq. (2) (dash-dotted line) for (a) γ =0.5, (b) 1.5, (c) 5.0, and (d) 10.

calculated with the YI formula tend to become less pronounced, and the entire $n_e(t)$ profiles converge to $n_e(t)$ dependences calculated with the use of the PPT model [cf. the solid and dashed curves in Fig. 2(b)]. Conversely, if formally extended to the $\gamma>1$ regime (the quasistatic approach is inapplicable in this range), Eq. (2) for the ionization rate would yield sharp steps in the $n_e(t)$ profile even for $\gamma>1$ [the dash-dotted line in Fig. 2(b)], where no sensitivity to the phase of the laser field should be expected from general physical arguments.

For realistic conditions of high-field laser experiments, when the radial profile of field intensity across a laser beam should be taken into consideration, analysis of the temporal wave form and the spectral properties of the field behind the interaction region should include integration over the beam profile (this procedure is also included in our modeling), with the field intensity varying from low values (corresponding to low γ) at the periphery of the laser beam to high values (corresponding to transition-range or even large γ) on the beam axis. Thus, even when the quasistatic approximation adequately describes the ionization rate in the most intense, central part of the beam, it does not guarantee, as confirmed by numerical simulations presented below, from inaccuracies in calculations of spectral and temporal characteristics for the entire beam as the quasistatic approximation fails at the periphery of the beam, where the field intensity is low.

III. RESULTS AND DISCUSSION: UNDERSTANDING EFFECTS RELATED TO ELECTRON TUNNELING IN THE EVOLUTION OF FEW-CYCLE LIGHT PULSES

We now proceed with modeling the evolution of intense few-cycle light pulses in an ionizing medium by solving the pulse propagation Eq. (1) with the ionization rate calculated with the YI formula and the quasistatic approach based on

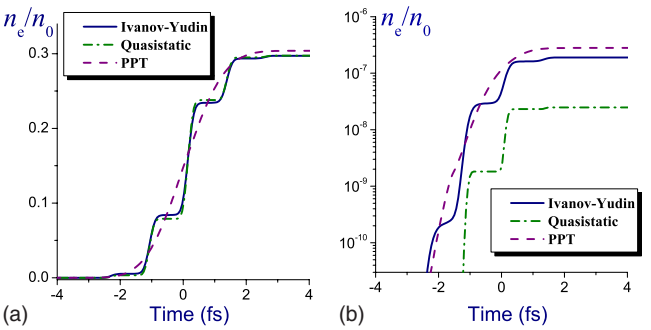

FIG. 2. (Color online) Temporal profiles of the electron density induced by a 5 fs pulse calculated by using the Yudin-Ivanov (solid line) formula, the PPT model (dashed line), and the quasistatic approximation (dash-dotted line). The central wavelength of the laser pulse is 750 nm. The peak intensity of the laser pulse is (a) 8×10^{14} W/cm^2 and (b) 10^{14} W/cm^2. The corresponding Keldysh parameter is (a) γ=0.5 and (b) 1.4.

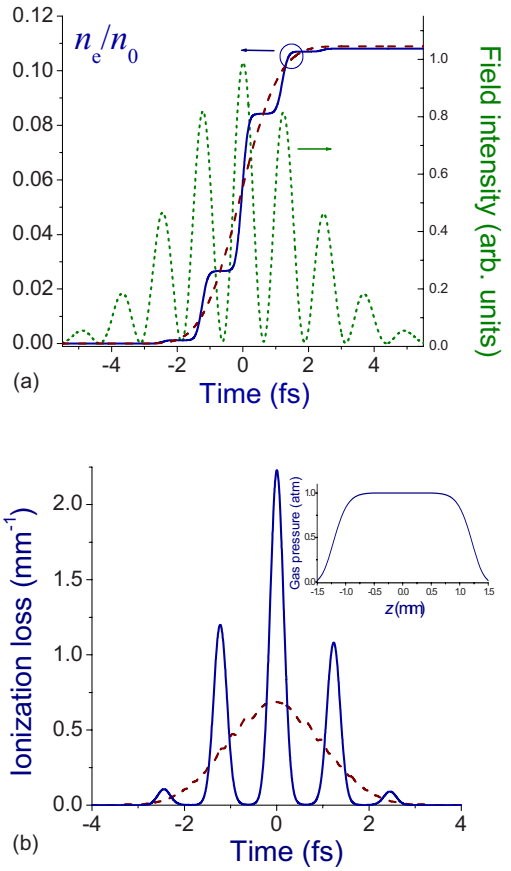

FIG. 3. (Color online) (a) Field intensity in a few-cycle laser pulse (dotted line) and the buildup of the electron density calculated with the use of the YI (solid line) and PPT (dashed line) formulas for the ionization rate. (b) Ionization loss $\alpha_p \propto I_p \partial n_e/\partial t$ calculated with the use of the YI (solid line) and PPT (dashed line) formulas for the ionization rate. The spatial profile of the gas pressure in the gas jet is shown in the inset. The maximum pressure of neon in a gas jet is 0.3 bar.

Eq. (2). Comparison of these simulations with the predictions of pulse-evolution modeling where $w(t)$ is calculated with the field-phase-insensitive Keldysh-type PPT formula [25] will help us identify the signatures related to attosecond electron tunneling in pulse propagation dynamics. The input laser pulse in our simulations is chosen in such a way [the dashed line in Fig. 3(a)] as to mimic a typical output of a Ti:sapphire laser compressed to a few-cycle pulse width by using a gas-filled capillary waveguide and a chirped-mirror compressor [10]. The input pulse energy is taken equal to 0.3 mJ. The initial pulse width is set equal to 5 fs. The radial field intensity profile across the laser beam is assumed to be Gaussian, with the peak, on-axis intensity corresponding to the Keldysh parameter $\gamma=0.5$. Dependence of the gas pressure on the propagation coordinate z [the inset to Fig. 3(b)] is chosen to model the spatial profile of the gas pressure in a gas-jet target. The laser beam is focused into the gas jet with a 1-m-focal-length lens. The temporal profiles of the electron density calculated for these parameters using the YI and PPT formulas for the ionization rate are shown, respectively, by the solid and dashed lines in Fig. 3(a).

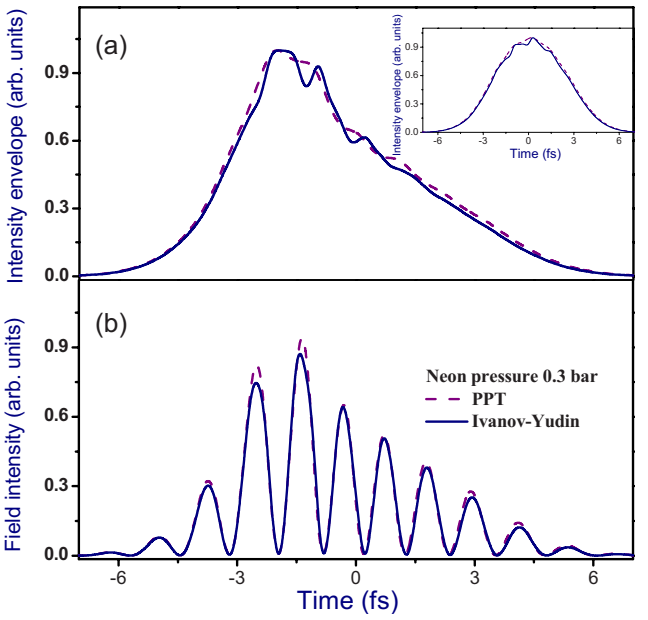

FIG. 4. (Color online) Intensity envelope (a) and the instantaneous field intensity (b) on the beam axis in a pulse transmitted through the gas jet. The ionization rate is calculated by using the Yudin-Ivanov (solid line) and Popov-Perelomov-Terentyev (dashed line) formulas. The pressure of neon in a gas jet is 0.3 bar. The inset shows the intensity envelope in a pulse transmitted through the gas jet integrated over the beam with the YI (solid line) and PPT (dashed line) formula for the ionization rate.

We distinguish between two physical mechanisms whereby ultrafast modulation of the plasma current translates into detectable features in the evolution of a few-cycle pulse. The first mechanism involves the pump-induced plasma loss $\alpha_p \propto I_p \partial n_e/\partial t$, described by the first term on the right-hand side of Eq. (1). This mechanism maps the temporal profile of $\partial n_e/\partial t$ onto the transmission of the ionizing medium. In the regime of tunneling ionization, pulse transmission becomes a phase-sensitive function of time [the solid line in Fig. 3(b)], whose peaks are locked to the peaks of the laser field [cf. Figs. 3(a) and 3(b)], which imposes an ultrafast, $\propto \partial n_e/\partial t$ amplitude modulation of the field wave form (Figs. 4 and 5) and gives rise to the generation of odd harmonics in the spectrum of the laser field transmitted through an ionizing gas (Figs. 6 and 7).

The second mechanism is accounted for by the plasma-current term, appearing as the last term on the right-hand side of Eq. (1), and is related to an effective nonlinear phase shift $\Delta\Phi=\omega_0 \delta n_p \Delta z/c$ of the probe field induced by an ultrafast modulation of the plasma current within a small propagation length Δz, with c being the speed of light in vacuum, $\delta n_p \approx -\omega_p^2/(2\omega_0^2)$, ω_p being the plasma frequency. Since $\omega_p^2 \propto n_e(t)$, this phase mask follows the temporal profile of $n_e(t)$, displaying stepwise changes locked to oscillations of the laser field. In the spectral domain, these steps of $n_e(t)$ translate into peaks at the frequencies of odd harmonics of ω_0.

Important general tendencies in the evolution of high-intensity few-cycle light pulses in a fast-ionizing gas (neon) are illustrated by spatiotemporal maps of the field transmit-

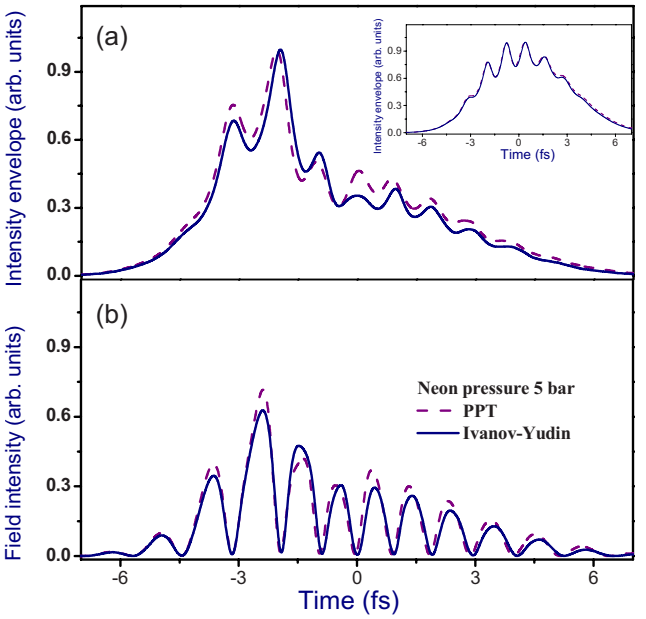

FIG. 5. (Color online) Intensity envelope (a) and the instantaneous field intensity (b) on the beam axis in a pulse transmitted through the gas jet. The ionization rate is calculated by using the Yudin-Ivanov (solid line) and Popov-Perelomov-Terentyev (dashed line) formulas. The pressure of neon in a gas jet is 5 bar. The inset shows the intensity envelope in a pulse transmitted through the gas jet integrated over the beam with the YI (solid line) and PPT (dashed line) formula for the ionization rate.

ted through the gas jet presented in Figs. 6 and 7. It can be seen from these maps that the leading edge of the pulse ionizes the gas, giving rise to a modulation of the central part of the pulse and inducing beam defocusing on the trailing edge of the pulse. In the regime of tunneling ionization with $w(t)$ calculated by using the YI formula, the steps in $n_e(t)$, locked to field half-cycles [Fig. 3(a)], induce a periodic shortening of field cycles, which is especially well pronounced in the central, most intense part of the pulse and on or near the beam axis [Fig. 6(a)], where the field has the highest intensity, leading to high rates of electron tunneling. A similar spatiotemporal dynamics has been earlier observed for longer, 20–25 fs laser pulses in a model where the ionization rate was calculated with the use of the quasistatic-approximation nonadiabatic ADK formula [22].

While each such cycle compression corresponds to spectral blueshifting, a periodic occurrence of such cycle shortening with a period equal to the field half-cycle translates into the generation of odd harmonics. Harmonics induced by plasma-current modulation related to electron tunneling are observed in the spectrum of the output field against a background of harmonics generated through a standard mechanism involving atomic nonlinear-optical susceptibilities, described by the $\propto P_{NL}$ term in Eq. (1). To quantify the significance of the above-specified harmonic-generation mechanisms, we represent the Fourier transform of the field in Eq. (1) as $E(z,r,\omega)=\hat{F}\{E(z,r,t)\}=F(z,r,\omega)e^{i\phi(z,r,\omega)}$ and introduce Fourier amplitudes and phases of the above-specified plasma-current and nonlinear susceptibility harmonic-generating terms in Eq. (1) by representing these terms as

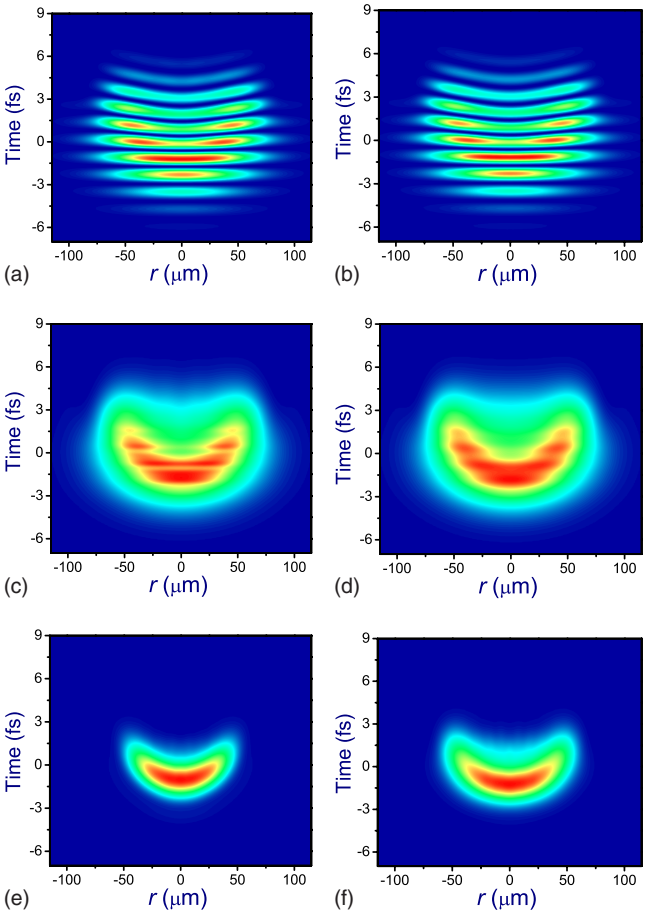

FIG. 6. (Color online) Spatiotemporal maps of (a) and (b) the field intensity, (c) and (d) intensity envelope, and (e) and (f) intensity envelope of the third harmonic in a pulse transmitted through the gas jet. The ionization rate is calculated by using the Yudin-Ivanov [(a), (c), and (e)] and Popov-Perelomov-Terentyev [(b), (d), and (f)] formulas. The pressure of neon in a gas jet is 0.3 bar.

$$P(z,r,\omega)e^{i\phi_\chi(z,r,\omega)}=\frac{\omega\chi^{(3)}_{\mathrm{THG}}}{c}\hat{F}\{E^3(z,r,t)\}, \tag{3}$$

$$I(z,r,\omega)e^{i\phi_p(z,r,\omega)}=\frac{1}{\omega c}\hat{F}\{\omega_p^2(z,r,t)E(z,r,t)\}, \tag{4}$$

$$L(z,r,\omega)e^{i\phi_l(z,r,\omega)}=\hat{F}\left\{\frac{I_p}{I(z,r,t)}\frac{\partial n_e(z,r,t)}{\partial t}E(z,r,t)\right\}, \tag{5}$$

where $\chi^{(3)}_{\mathrm{THG}}$ is the nonlinear susceptibility responsible for third-harmonic generation.

The field-evolution equation [Eq. (1)] then yields the following expression for the energy of the field contained within a spectral interval from ω_1 to ω_2,

$$W(z)=W_\chi(z)+W_p(z)+W_l(z), \tag{6}$$

where

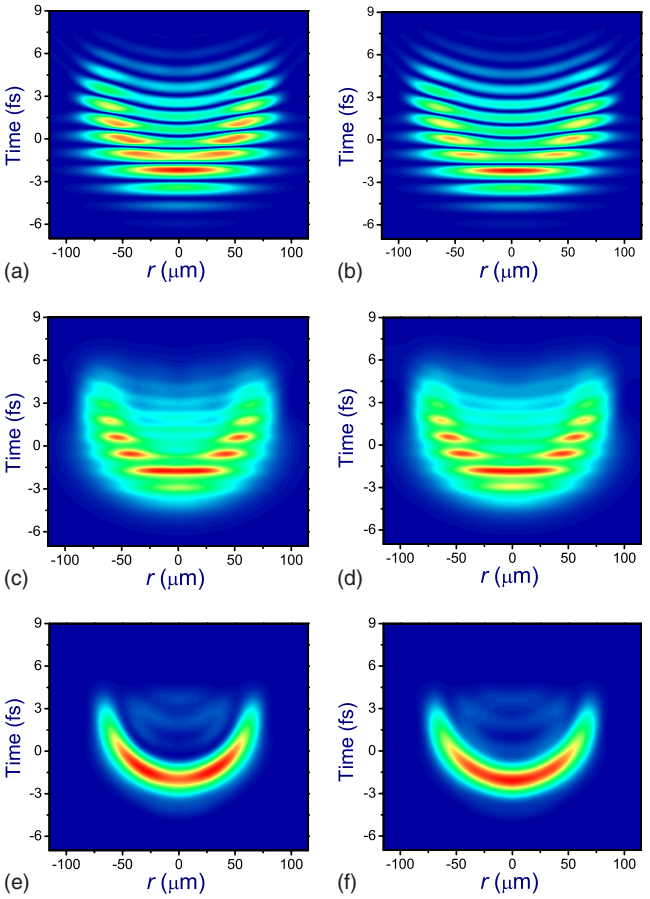

FIG. 7. (Color online) Spatiotemporal maps of (a) and (b) the field intensity, (c) and (d) intensity envelope, and (e) and (f) intensity envelope of the third harmonic in a pulse transmitted through the gas jet. The ionization rate is calculated by using the [(a), (c), and (e)] Yudin-Ivanov and [(b), (d), and (f)] Popov-Perelomov-Terentyev formulas. The pressure of neon in the gas jet is 5 bar.

$$W_\chi(z) = 2\pi\mu_0\omega c \int_0^z dz \int_{\omega_1}^{\omega_2} d\omega \int_0^\infty FP \sin(\phi - \phi_\chi) r dr, \tag{7}$$

$$W_p(z) = 2\pi \int_0^z dz \int_{\omega_1}^{\omega_2} d\omega \int_0^\infty FI \sin(\phi_p - \phi) r dr, \tag{8}$$

$$W_l(z) = -2\pi \int_0^z dz \int_{\omega_1}^{\omega_2} d\omega \int_0^\infty FL \cos(\phi_l - \phi) r dr. \tag{9}$$

We now define the third harmonic as radiation emitted within the wavelength range from $\lambda_1 = 2\pi c/\omega_2 = 180$ nm to $\lambda_2 = 2\pi c/\omega_1 = 330$ nm. Figures 8(a) and 8(b) present the energies W_χ, W_p, and W_l of partial third-harmonic fields generated by different nonlinear mechanisms calculated as functions of the propagation distance z. The total energy calculated as a sum in Eq. (6) [the solid line in Figs. 8(a) and 8(b)] agrees very well with the energy of the third-harmonic signal found directly from the numerical solution of Eq. (1) with the YI formula for the ionization rate [open circles in Figs. 8(a) and 8(b)]. For comparison, we also plot in Figs. 8(a) and 8(b) the results of simulations performed with the ionization rate calculated using the PPT formula (filled circles). At low gas pressures, as can be seen from Fig. 8(a), the third harmonic generated due to plasma density modulation is much more intense than the third harmonic related to the atomic susceptibility. As the gas pressure grows, the role of susceptibility-induced harmonics increases [Fig. 8(b)]. The growth in the gas pressure, on the other hand, also increases the phase mismatch between the third-harmonic field and the third-order nonlinear polarization. As a result, the third-harmonic signal can display a nonmonotonic behavior as a function of the gas pressure, seen for W_χ in Fig. 9, leaving much room for the optimization of frequency conversion of few-cycle laser pulses. Calculations presented in Fig. 9 also suggest that increasing the gas pressure does not automatically enhance the harmonic yield for a given propagation path of a light pulse in a gas medium. In the high-pressure regime (above 10 bar in Fig. 9), the propagation path should often be reduced in order to avoid phase-mismatching effects.

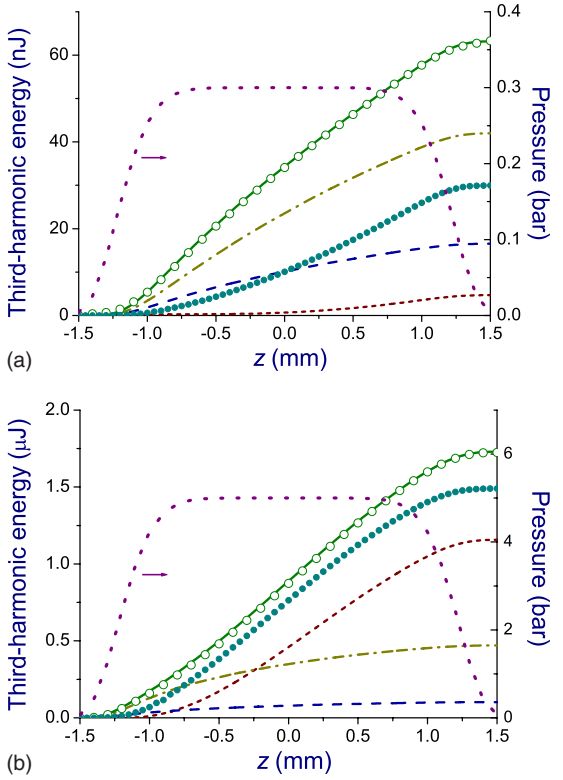

FIG. 8. (Color online) The total energy of the third harmonic (open circles) and the energies W_χ (dotted line), W_p (dashed line), and W_l (dash-dotted line) of partial third-harmonic fields generated by different nonlinear mechanisms calculated as functions of the propagation distance z with the YI formula for the ionization rate. The solid line represents the sum $W = W_\chi + W_p + W_l$. Filled circles show the results of simulations with the PPT formula for the ionization rate. The spatial profile of neon pressure in the gas jet is shown by the dotted line. The maximum neon pressure in the gas jet is 0.3 bar (a) and 5 bar (b).

With ionization-induced defocusing substantially lowering the field intensity on the trailing edge of the laser pulse

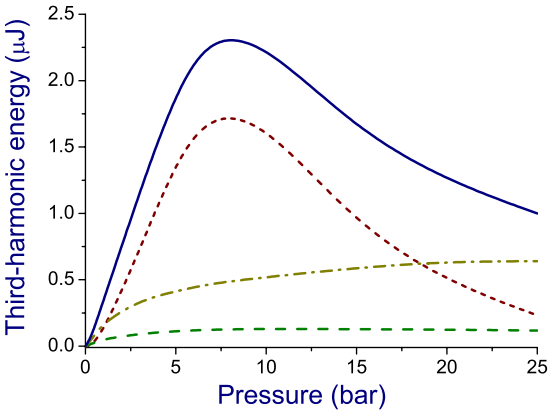

FIG. 9. (Color online) The total energy of the third harmonic (solid line) and the energies W_χ (dotted line), W_p (dashed line), and W_I (dash-dotted line) of partial third-harmonic fields generated by different nonlinear mechanisms calculated as functions of the gas pressure in the gas jet with the YI formula for the ionization rate.

(Figs. 6 and 7), the third-harmonic field is much better localized in the time domain than the laser field is. Because of the radially nonuniform group delay introduced by plasma dispersion, the third harmonic forms a crescent-shaped pattern on the *r*-*t* plane (Figs. 6 and 7), suggesting the possibility of ultrashort pulse generation in the uv range with an appropriate technique for spatial chirp compensation [29]. In the low-pressure regime, third-harmonic pulses generated by ultrafast plasma density modulation [Fig. 6(e)] are typically substantially shorter than third-harmonic pulses produced due to atomic susceptibilities [Fig. 6(f)].

Since the electron density is nonuniform across the laser beam, the shortest third-harmonic pulses [Fig. 6(e)] and the most clearly resolved pulse wave form modulation [Figs. 4(a) and 4(b)] are obtained on and near the axis of the laser beam. Integration over the beam leads to longer third-harmonic pulses [Fig. 6(a)] and dramatically lowers the visibility of electron-tunneling-induced modulation of the field wave form (the inset in Fig. 4). In the high-pressure regime, the signatures of tunneling ionization in the field wave form, which can still be observed on the beam axis [Figs. 5(a) and 5(b)], become completely unresolvable after the integration over the beam (the inset in Fig. 5).

In Figs. 10(a) and 10(b), we compare the spectra of high-intensity few-cycle light pulses behind a gas jet simulated by numerically solving Eq. (1) with $w(t)$ calculated with the YI and PPT formulas and integrating the result over the beam. It can be seen from Figs. 10(a) and 10(b) that the spectra calculated with these two approaches agree perfectly well within their visible and near-infrared parts. The high-frequency tails of these spectra, however, exhibit appreciable differences. Since the PPT formalism leads to a Keldysh-type, cycle-averaged expression for $w(t)$, it cannot account for an ultrafast modulation of the electron density. As a result, the high-frequency wings of the spectra calculated with the use of this formalism [shown by the dashed line in Figs. 10(a) and 10(b)] can only display harmonic signals due to atomic susceptibilities. On the contrary, the pulse evolution

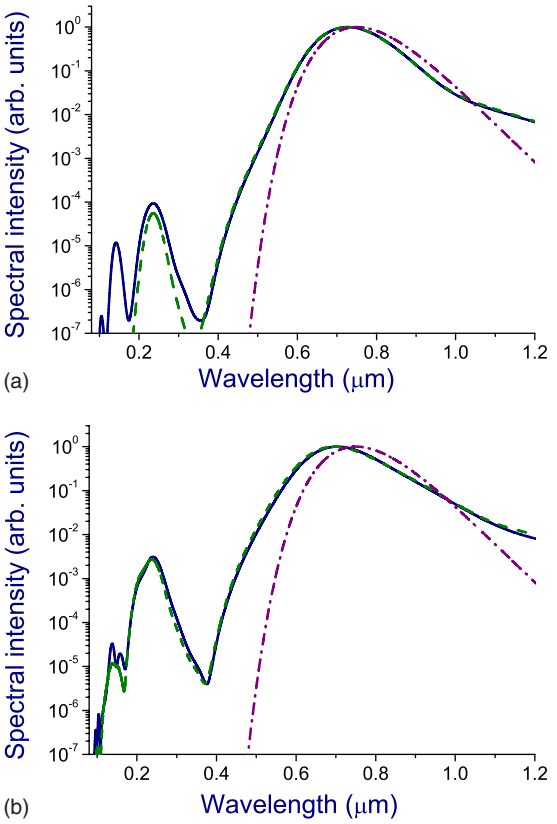

FIG. 10. (Color online) The spectra of few-cycle laser pulses transmitted through the gas jet with a neon pressure of (a) 0.3 bar and (b) 5 bar. The ionization rate is calculated using the YI (solid line) and PPT (dashed line) formulas. The dash-dotted line shows the input spectrum of the laser pulse.

equation with the YI formula for $w(t)$ predicts odd-harmonic generation due to both atomic susceptibilities and ultrafast plasma-current modulation [solid line in Figs. 10(a) and 10(b)]. The difference between the harmonic spectra calculated with the use of these two approaches is especially striking in the regime of low gas pressures [Fig. 10(a)], where the atomic susceptibilities are too low to generate detectable harmonic signals. In the time domain, these signatures of electron tunneling are observed as a fast modulation of the field wave form, leading to qualitative differences, both on beam axis [Fig. 4(a)] and for the entire beam (the inset in Fig. 4), from the predictions of a pulse-evolution model where the ionization rate is calculated with the PPT formula (see Figs. 4 and 6). For high gas pressures, on the other hand, harmonic generation, as can be seen from Figs. 8(b) and 9, is dominated by atomic susceptibilities. In this regime, optical nonlinearities related to ionization and atomic susceptibilities tend to broaden the spectra of the driving pulse and its harmonics to such an extent that different parts of the spectrum merge together, giving rise to a supercontinuum stretching from the deep uv to the infrared [Fig. 10(b)]. With the nonlinear response of a high-pressure gas dominated by atomic susceptibilities and ionization effects being nonuniform across the beam (Figs. 5 and 7), pulse-evolution models with

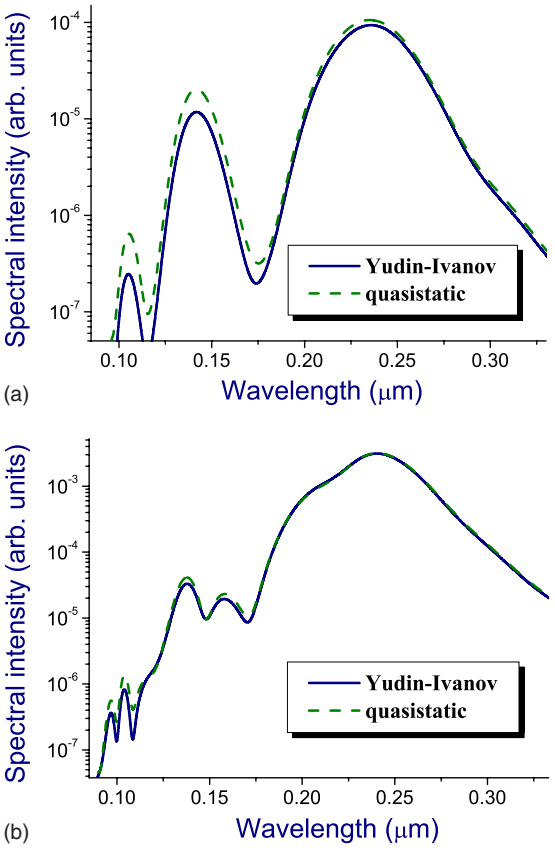

FIG. 11. (Color online) The spectra of few-cycle laser pulses transmitted through the gas jet with a neon pressure of (a) 0.3 bar and (b) 5 bar. The ionization rate is calculated using the YI formula (solid line) and the quasistatic approximation (dashed line).

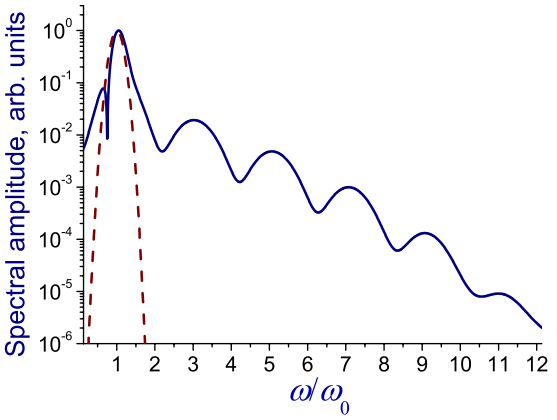

FIG. 12. (Color online) The spectrum of optical harmonics (Fourier transform of the field as a function of frequency) generated due to electron density modulation within a propagation length of 0.1 mm. A neon pressure is 0.3 bar. The Keldysh parameter is $\gamma = 0.5$. The dashed line shows the spectrum of the input laser pulse.

YI and PPT ionization rates tend to give converging predictions for the beam-integrated spectra [Fig. 10(b)] and field wave forms [inset in Fig. 5(b)] of few-cycle pulses. Under these conditions, it becomes difficult to separate the signatures of tunneling ionization in harmonic spectra and in field wave forms from effects related to atomic susceptibilities. Due to the difference in phase matching, such a separation becomes possible, as shown by recent experiments [28], in a noncollinear pump-probe scheme, where a high-intensity pump is used to induce electron tunneling in a medium, while a weaker noncollinear probe pulse reads out the electron density modulation, acquiring phase and amplitude modulation, which can be detected as optical harmonic signals.

In Figs. 11(a) and 11(b), we compare the spectra of few-cycle laser pulses behind a gas jet calculated with the use of the YI formula and the quasistatic-approximation results of Eq. (2). In the low-pressure regime [a neon pressure of 0.3 bar, Fig. 11(a)], where harmonic generation is dominated by the modulation of the plasma density, sharper steps in the $n_e(t)$ profile predicted by the quasistatic approximation translate into more intense optical harmonics [the dashed line in Fig. 11(a)]. Thus, in this regime, the quasistatic approximation noticeably overestimates the amplitude of harmonics in the spectrum of the output signal. In the high-pressure regime [a neon pressure of 5 bar, Fig. 11(b)], harmonics are generated mainly through atomic nonlinear susceptibilities. As a consequence, the output spectra are not very sensitive to the details of ionization process. In this regime, simulations performed with the YI formula and the quasistatic-approximation expression for the ionization rate give converging results [cf. the solid and dashed lines in Fig. 11(b)].

In the discussion above, we restricted our analysis to low-order (third, fifth, and seventh) optical harmonics generated due to electron density modulation in the spectral range from approximately 100 to 360 nm (Figs. 10 and 11). Since for harmonics generated by tunneling electrons, the harmonic amplitude falls off much faster as a function of the harmonic number than it does in the spectrum of harmonics generated by the electron rescattering mechanism [30], detection of high-order harmonics related to electron tunneling becomes very difficult if possible at all, as the latter are masked by harmonics emitted through electron rescattering, which tend to form a broad plateau. Indeed, only low-order (from the third to the seventh) optical harmonics have been experimentally detected so far in the regime where harmonic generation is predominantly due to electron tunneling [28]. In Fig. 12, we plot the spectrum of optical harmonics (Fourier transform of the field as a function of frequency) generated by a few-cycle light pulse within a very small propagation path of only 0.1 mm inside an ionizing gas. The spectrum of optical harmonics displays no plateau in this case, rapidly falling of to very low levels already for the ninth and 11th harmonics. In this calculation, we deliberately keep the propagation length short in order to reduce the influence of propagation effects, which typically complicate the map between the temporal dynamics of tunneling ionization and harmonic spectra. When propagation effects included in simulations, it becomes even more difficult to isolate low-intensity high-order harmonics generated by tunneling electrons from harmonics emitted by rescattering electrons.

IV. CONCLUSION

Numerical simulations presented in this paper demonstrate that the sensitivity of electron tunneling to the phase of an ionizing light field is manifested in specific features and tendencies in the spectral and temporal evolution of intense few-cycle light pulses. An ultrafast buildup of the electron density in the regime of tunneling ionization is shown to modulate a wave form of a few-cycle field, enhance the short-wavelength part of its spectrum, and generate odd-order optical harmonics. All these effects should be included in accurate models of filamentation and supercontinuum generation by intense few-cycle laser pulses. In a low-pressure gas, the signatures of electron tunneling in the evolution of few-cycle pulses are especially well resolved and can be employed to map attosecond electron tunneling dynamics.

ACKNOWLEDGMENTS

Stimulating discussions with E. Goulielmakis, U. Graf, F. Krausz, and T. Fuji are gratefully acknowledged. This study was supported in part by the Russian Foundation for Basic Research (Projects No. 08-02-91756, No. 08-02-92226, No. 08-02-92009, No. 09-02-12359, and No. 09-02-12373) and the Federal Program of the Russian Ministry of Education and Science (Contracts No. 1130 and 02.740.11.0223). A part of this research was done in the framework of the COST MP0702 action, supported by the European Science Foundation.

[1] L. Bergé, S. Skupin, R. Nuter, J. Kasparian, and J.-P. Wolf, Rep. Prog. Phys. **70**, 1633 (2007).
[2] A. Couairon and A. Mysyrowicz, Phys. Rep. **441**, 47 (2007).
[3] T. Brabec and F. Krausz, Rev. Mod. Phys. **72**, 545 (2000).
[4] P. B. Corkum, C. Rolland, and T. Srinivasan-Rao, Phys. Rev. Lett. **57**, 2268 (1986).
[5] *The Supercontinuum Laser Source*, edited by R. Alfano (Springer, New York, 1989).
[6] *Supercontinuum Generation*, edited by A. M. Zheltikov, special issue of Appl. Phys. B: Lasers Opt. **77** (2/3) (2003).
[7] A. Braun, G. Korn, X. Liu, D. Du, J. Squier, and G. Mourou, Opt. Lett. **20**, 73 (1995).
[8] D. J. Cook and R. M. Hochstrasser, Opt. Lett. **25**, 1210 (2000).
[9] T. Bartel, P. Gaal, K. Reimann, M. Woerner, and T. Elsaesser, Opt. Lett. **30**, 2805 (2005).
[10] E. Goulielmakis, V. S. Yakovlev, A. L. Cavalieri, M. Uiberacker, V. Pervak, A. Apolonski, R. Kienberger, U. Kleineberg, and F. Krausz, Science **317**, 769 (2007).
[11] P. B. Corkum and F. Krausz, Nat. Phys. **3**, 381 (2007).
[12] J. Kasparian, M. Rodriguez, G. M'ejean, J. Yu, E. Salmon, H. Wille, R. Bourayou, S. Frey, Y. B. Andre, A. Mysyrowicz, R. Sauerbrey, J. P. Wolf, and L. Woeste, Science **301**, 61 (2003).
[13] C. P. Hauri, W. Kornelis, F. W. Helbing, A. Heinrich, A. Couairon, A. Mysyrowicz, J. Biegert, and U. Keller, Appl. Phys. B: Lasers Opt. **79**, 673 (2004).
[14] T. Fuji, T. Horio, and T. Suzuki, Opt. Lett. **32**, 2481 (2007).
[15] U. Graf, M. Fieß, M. Schultze, R. Kienberger, F. Krausz, and E. Goulielmakis, Opt. Express **16**, 18956 (2008).
[16] M. Geissler, G. Tempea, A. Scrinzi, M. Schnürer, F. Krausz, and T. Brabec, Phys. Rev. Lett. **83**, 2930 (1999).
[17] A. L. Gaeta, Phys. Rev. Lett. **84**, 3582 (2000).
[18] L. V. Keldysh, Zh. Eksp. Teor. Fiz. **47**, 1945 (1964) [Sov. Phys. JETP **20**, 1307 (1965)].
[19] G. L. Yudin and M. Yu. Ivanov, Phys. Rev. A **64**, 013409 (2001).
[20] T. Brabec and F. Krausz, Phys. Rev. Lett. **78**, 3282 (1997).
[21] E. Priori, G. Cerullo, M. Nisoli, S. Stagira, S. De Silvestri, P. Villoresi, L. Poletto, P. Ceccherini, C. Altucci, R. Bruzzese, and C. de Lisio, Phys. Rev. A **61**, 063801 (2000).
[22] C. Altucci, R. Esposito, V. Tosa, and R. Velotta, Opt. Lett. **33**, 2943 (2008).
[23] M. V. Ammosov, N. B. Delone, and V. P. Krainov, Zh. Eksp. Teor. Fiz. **91**, 2008 (1986) [Sov. Phys. JETP **64**, 1191 (1986)].
[24] M. Uiberacker, Th. Uphues, M. Schultze, A. J. Verhoef, V. Yakovlev, M. F. Kling, J. Rauschenberger, N. M. Kabachnik, H. Schroder, M. Lezius, K. L. Kompa, H.-G. Muller, M. J. J. Vrakking, S. Hendel, U. Kleineberg, U. Heinzmann, M. Drescher, and F. Krausz, Nature (London) **446**, 627 (2007).
[25] A. M. Perelomov, V. S. Popov, and M. V. Terent'ev, Zh. Eksp. Teor. Fiz. **50**, 1393 (1966) [Sov. Phys. JETP **23**, 924 (1966)].
[26] W. M. Wood, C. W. Siders, and M. C. Downer, IEEE Trans. Plasma Sci. **21**, 20 (1993).
[27] F. Brunel, J. Opt. Soc. Am. B **7**, 521 (1990).
[28] A. J. Verhoef, A. Mitrofanov, E. E. Serebryannikov, D. Kartashov, A. M. Zheltikov, and A. Baltuška, *Ultrafast Phenomena* (Springer, Heidelberg, 2009); in *Frontiers in Optics*, OSA Technical Digest (CD) (Optical Society of America, Washington, D.C., 2008), paper FThH3.
[29] E. E. Serebryannikov, E. Goulielmakis, and A. M. Zheltikov, New J. Phys. **10**, 093001 (2008).
[30] P. B. Corkum, Phys. Rev. Lett. **71**, 1994 (1993).